PLOS ONE

RESEARCH ARTICLE

Comparative proteomic analysis of Gib2 validating its adaptor function in *Cryptococcus neoformans*

Gillian O. Bruni[1], Blake Battle[2], Ben Kelly[1], Zhengguang Zhang[3], Ping Wang[1,4]*

1 Department of Microbiology, Immunology, and Parasitology, Louisiana State University Health Sciences Center, New Orleans, LA, United States of America, **2** College of Arts and Sciences, Loyola University New Orleans, New Orleans, LA, United States of America, **3** Department of Plant Pathology, College of Plant Protection, Nanjing Agricultural University, Nanjing, China, **4** Department of Pediatrics, Louisiana State University Health Sciences Center, New Orleans, LA, United States of America

* pwang@lsuhsc.edu

Citation: Bruni GO, Battle B, Kelly B, Zhang Z, Wang P (2017) Comparative proteomic analysis of Gib2 validating its adaptor function in *Cryptococcus neoformans*. PLoS ONE 12(7): e0180243. https://doi.org/10.1371/journal.pone.0180243

Editor: Yong-Sun Bahn, Yonsei University, REPUBLIC OF KOREA

Received: March 25, 2017

Accepted: June 12, 2017

Published: July 7, 2017

Data Availability Statement: All relevant data are within the paper and its Supporting Information files.

Funding: This work is supported by US NIH grants AI121460 and AI121451 and Natural Science Foundation of China grants 31530063 and 31325022Z. Z. Zhang is also supported by an especially appointed professorship from Jiangsu, China.

Competing interests: The authors have declared that no competing interests exist.

Abstract

Cryptococcus neoformans causes often-fatal fungal meningoencephalitis in immunocompromised individuals. While the exact disease mechanisms remain elusive, signal transduction pathways mediated by key elements such as G-protein α subunit Gpa1, small GTPase Ras1, and atypical Gβ-like/RACK1 protein Gib2 are known to play important roles in *C. neoformans* virulence. Gib2 is important for normal growth, differentiation, and pathogenicity, and it also positively regulates cAMP levels in conjunction with Gpa1. Interestingly, Gib2 displays a scaffold protein property by interacting with a wide variety of cellular proteins. To explore Gib2 global regulatory functions, we performed two-dimensional differential gel electrophoresis (DIGE) analysis and found that *GIB2* disruption results in an increased expression of 304 protein spots (43.4%) and a decreased expression of 396 protein spots (56.6%). Analysis of 96 proteins whose expression changes were deemed significant ($\geq$ +/- 1.5- fold) revealed that 75 proteins belong to at least 12 functional protein groups. Among them, eight groups have the statistical stringency of $p \leq 0.05$, and four groups, including Hsp70/71 heat shock protein homologs and ribosomal proteins, survived the Bonferroni correction. This finding is consistent with earlier established roles for the human Gβ-like/RACK1 and the budding yeast *Saccharomyces cerevisiae* Asc1. It suggests that Gib2 could also be part of the complex affecting ribosomal biogenesis and protein translation in *C. neoformans*. Since eukaryotic Hsp70/71 proteins are involved in the facilitation of nascent protein folding, processing, and protection of cells against stress, we also propose that Gib2-regulated stress responses are linked to fungal virulence. Collectively, our study supports a conserved role of Gβ-like/RACK/Gib2 proteins in the essential cellular process of ribosomal biogenesis and protein translation. Our study also highlights a multifaceted regulatory role of Gib2 in the growth and pathogenicity of *C. neoformans*.

Introduction

Cryptococcus neoformans is a basidiomycetous fungal pathogen that has a predilection for the human central nervous system causing meningoencephalitis in individuals with a compromised immune status. Virulence of the fungus is multifaceted depending on many factors, including, but not limiting to, the ability to grow at the host body temperature, elaborate the melanin pigment and a polysaccharide capsule, and produce proteinases such as ureases and phospholipases (reviewed by [1]).

Guanine nucleotide binding protein (G-protein)-mediated signal transduction pathways are one of the most important mechanisms by which eukaryotic cells sense extracellular signals and integrate them via intrinsic signals or pathways, such as cAMP or the MAP kinase pathways (reviewed in [2]). In *C. neoformans*, three Gα protein subunits Gpa1, Gpa2, and Gpa3 function in two distinct signaling pathways [3]. Gpa1, adenylyl cyclase Cac1, protein kinase A regulatory subunit Pkr1 and catalytic subunit Pka1, and Cac1 associated protein Aca1 govern a cAMP-dependent signaling pathway to directly impact fungal pathogenicity [4,5,6]. Meanwhile, Gpa2 and Gpa3 function in a distinct pathway(s) to regulate pheromone responsive mating and differentiation that is also to certain degree linked to virulence [3,7,8].

To understand mechanisms by which Gα Gpa1 exhibits its regulatory function in *C. neoformans*, we identified Gib2 as an atypical Gβ-like protein that not only couples with Gpa1 but also exhibits an ancillary role in cAMP signaling. Significantly, we discovered that Gib2 positively regulates cAMP signaling by countering the negative regulatory function of Ras1 upon Cac1 [9]. Moreover, we found that Gib2 interacts with many additional proteins such as protein kinase C (Pkc1), human intersectin homolog (Cin1), and various ribosomal subunits [9,10]. This ability of interacting with many proteins encoding important and diverse functions suggests that Gib2 could function as a critical regulator of physiology and pathogenicity in the fungus.

The human Gβ-like/RACK1 and the budding yeast *Saccharomyces cerevisiae* Asc1 proteins are important regulatory proteins for growth and differentiation that are also part of the ribosomal complex involved in ribosomal biogenesis and protein translation [11,12,13,14]. The Gib2 protein exhibits high amino acid sequence homology and certain functional similarity with Gβ-like/RACK1/Asc1 [9,10,15]. Indeed, our previous findings identified an association between Gib2 and ribosomal protein assembly [9]. To explore the global regulatory role of Gib2 in *C. neoformans*, we examined genome-wide targets of Gib2 by comparative proteomic analysis using two-dimensional difference gel electrophoresis (DIGE) coupled with mass spectrometry that yields novel findings.

Comparative proteomic analysis is a powerful tool that provides a qualitative and quantitative global expression profile, which is invaluable in gaining a systematic understanding of molecular processes involved in growth, development, and/or virulence [16,17]. The DIGE technique was evolved from two-dimensional electrophoresis (2-DE) that is one of the most sensitive and powerful techniques for separating hundreds of proteins [17,18]. DIGE greatly limits inter-gel variation of 2-DE and provides a wide application in proteomic studies examining changes in protein abundance, post-translational modifications, truncations and any modification that might change the size or isoelectric point of proteins [19,20]. The technique is well suited for our purposes. In the present study, we discovered that Gib2 has a global impact on protein expressions in *C. neoformans* as the disruption of the *GIB2* gene affected a wide array of proteins involved in various cellular processes. This includes ribosomal biogenesis, protein synthesis, stress tolerance, intracellular trafficking, amino acid and carbohydrate metabolism, and signal transduction. These findings are consistent with our proposition that

Gib2 has a multifaceted regulatory role important in the growth and pathogenicity of *C. neoformans*.

Materials and methods

Fungal strains, cultures and transformation

C. neoformans var. *grubii* (serotype A) archetype H99 [21] and the derivative *gib2* mutant [9] strains were maintained on yeast peptone dextrose (YPD) agar. The *gib2* mutant strain linked to the Nourseothricin resistance marker gene (*NAT*) was described previously [9].

Protein extraction and 2-DIGE

C. neoformans cells grown overnight in liquid YPD media at 30˚C were collected, washed, and resuspended in liquid yeast nitrogen base (YNB) and grown for an additional three hours. Cells were then harvested and fragmented with glass beads (0.4–0.5 mm) using a high-speed bead-beating homogenizer (FastPrep FP120). Supernatants were recovered and crude proteins were extracted with the TCA/acetone precipitation method following the standard protocol provided by BioRad with some modifications. Briefly, cells were resuspended in 500 μl lysis buffer containing 7 M urea, 2 M thiourea, 4% (w/v) CHAPS, 65 mM DTT, and 1 mM PMSF, and fragmented for 40 x 8 sec, with 3–5 min intervals for cooling. Insoluble materials were removed by precipitation for 15 min in a microfuge. Supernatants were then mixed with 500 μl of 10% (w/v) TCA/acetone (500 μl) containing 1 mM PMSF and 0.07% (w/v) β-mercaptoethanol. Following the precipitation, the pellets were washed, resuspended in lysis buffer, and protein concentrations were estimated using the standard Bradford method [22]. For the first dimension isoelectric focusing electrophoresis, approximately 1 g of protein from each strain was labeled and co-loaded on an 18 cm, pH 3–10 nonlinear gradient IPG strip (GE Healthcare) and separated.

The second gel electrophoresis was performed using 12% SDS-PAGE. Upon completion, proteins were stained with Coomassie Brilliant Blue G-250 and images digitalized with a Typhoon image scanner. Each scan revealed one of the CyDye signals (Cy3 and Cy5). Images were analyzed with ImageQuant software (GE Healthcare Life Sciences). Protein spots were detected, matched, and normalized on the basis of the total density of gels with the parameter of percent volume, according to the software guide. For each spot, the mean relative volume (RV) was computed at every sample. The spots showing a mean RV that changed more than 1.5- fold ($p < 0.05$) in different stages were considered differentially expressed proteins. Protein spots of interest were picked with an Ettan Spot Picker, and identified by mass spectrometry.

In-gel digestion, LC-MS/MS analysis, and database search

LC-MS/MS analysis, database search, and statistical analysis were provided by Appliced Biomics (Hayward, CA). Briefly, protein samples were reduced with dithiothreitol (DTT), alkylated with iodoacetamide, and digested with trypsin at 37˚C overnight. 5% formic acid was added to stop the digestion and the solvent was then evaporated in a speed vacuum [9]. The dried samples were suspended in 2% acetonitrile (containing 0.1% formic acid) and subjected to LC-electrospray ionization-MS/MS analysis on a Finnigan LTQ ion trap mass spectrometer (ThermoFinnigan, San Jose, CA) as described previously [9]. Briefly, each sample was loaded into a C_{18} trap column for desalting before being eluted into a reverse-phase C_{18} analytical column for LC separation and MS detection. The acquired raw data were processed using BioWorks (version 3.3) (Thermo Electron). Following protein identification, pathway analysis

and protein clustering were performed using the Database for Annotation, Visualization, and Integrated Discovery (DAVID, NIAID/NIH).

Semi-quantitative RT-PCR

Total RNA was extracted from the wild type H99 and the *gib2* mutant strains that were subject to the same induction condition as for protein extraction, using the Trizol reagent (Invitrogen, CA). Following digestion with RNase-free DNase (RQ1, Promega), RNA was quantified using a NanoVue Plus spectrophotometer (GE Life Sciences). One μg RNA was used for reverse transcription with random hexamers (SuperScript First Strand, Invitrogen). An equal amount of cDNA (200 μg) was used in PCR with gene-specific primer pairs. Primers PW1960/PW1961, PW1962/PW1963, PW1974/PW1965, PW1966/PW1967, and PW1614/PW1615 (S1 Fig) were used to amplify partial fragments of a Hsp70-like protein (spot 12, gi5826470), flavohemoglobin (spot 36, gi37783289), a glyoxal oxidase precursor (spot 3, gi58267754), 60S ribosomal protein L9 (spot 75, gi58258095), and β-actin (*ACT*) transcripts, respectively. Images of RT-PCR stained with GelRed (Biotium) were acquired with a Bio-Rad Gel Doc XR+ System (Bio-Rad), and bands were quantified using ImageJ. The band intensity was expressed as relative absorbance units using the constitutively expressed actin gene (*ACT*) as a control for normalization of initial variations in sample concentration and for reaction efficiency. Mean and standard deviation were calculated after normalization to actin and were plotted as previously described [23].

Results

Identification of proteins regulated by Gib2 through a proteome approach

We previously identified Gib2 as an atypical Gβ protein that couples to Gα Gpa1 and showed that Gib2 positively regulates cAMP signaling, in conjunction with Gpa1 [9]. We also found that Gib2 interacts with approximately 50 proteins, including the protein kinase C homolog Pkc1, the endocytic adaptor protein Cin1, and several ribosomal subunits [9,10]. To further understand the global regulatory role of Gib2, we performed DIGE on protein extracts from the *gib2* mutant and the wild-type strains of *C. neoformans*. Since the expression of *GIB2* can be further induced upon a brief incubation in nutrient-poor YNB medium [9], we included this incubation period following overnight growth in nutrient-rich YPD in order to maximize potential differentiations between the *gib2* mutant and the wild-type strains.

We have obtained high quality data based on the quality of protein samples and 2-D DIGE gel runs. In total, approximately 700 protein spots could be detected reproducibly, which were distributed mostly in the pH 5–7 range and with relative molecular masses of between 14 and 110 kDa (Fig 1). Quantitative image analysis of three replicates for each sample using PDQuest 7.2 software showed a total of 96 protein spots with equal to or more than 1.5- fold difference ($P < 0.05$) in expression values in the *gib2* mutant compared to the wild-type strain H99. The 96 spots were picked and subject to mass spectrometry analysis. 75 proteins were reliably identified following searching against the *C. neoformans* database. For the majority of the proteins identified, experimental molecular weight (Mr) and isoelectric point (pI) match the theoretical values of the corresponding proteins. However, differences between the experimental and theoretical values of MW and pI were also noticeable (spots 3 and 4, spots 16, 17, 30 and 31). This may suggest the presence of factors such as alternate isoforms of such proteins (e.g. mRNA splice variants) or post-translational modifications.

Interestingly, of the 75 proteins identified, nearly the half (38) was decreased and the other half (37) increased in abundance in the *gib2* mutant (Fig 2), suggesting that the Gib2 protein has both positive and negative regulatory roles in *C. neoformans*. Based on their putative cellular functions, these 75 proteins were further grouped into 12 functional classes: heat shock

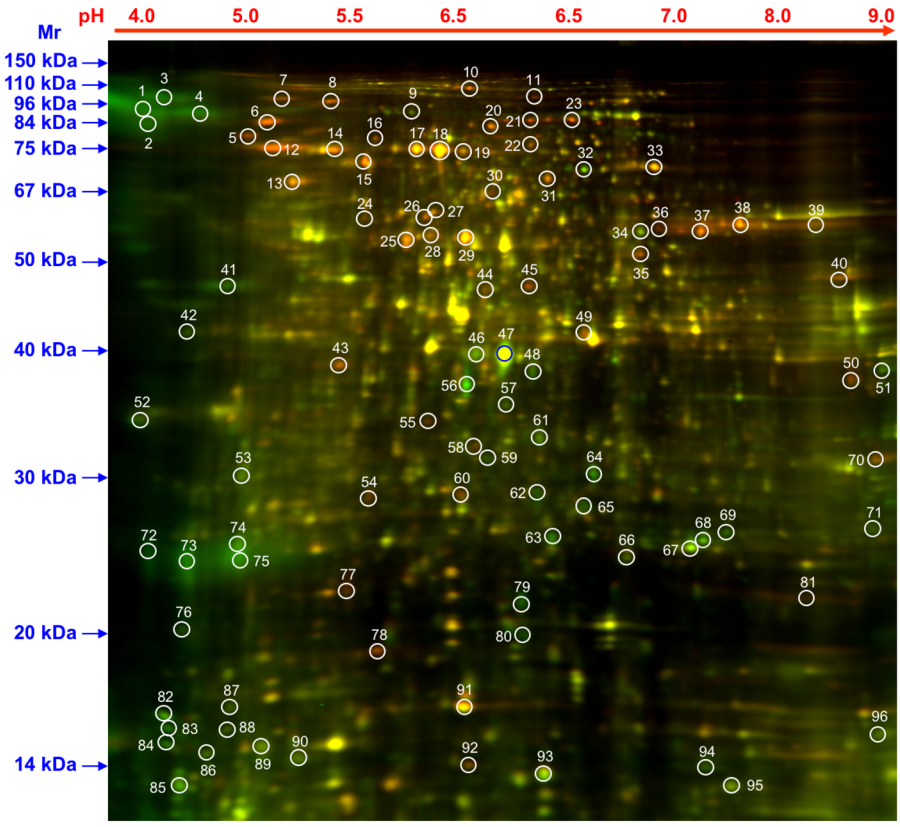

Fig 1. Two-dimensional gel electrophoresis (2-DIGE) of *C. neoformans* wild type and *gib2* mutant strains. Strains were cultured overnight in liquid YPD medium at 30˚C followed by an additional three-hour incubation in YNB. Crude proteins were extracted using glass beads and a homogenizer, precipitated with TCA/acetone, normalized, labeled, and subjected to 2-DIGE. The numbered circles indicate the differentially expressed and identified protein spots.

https://doi.org/10.1371/journal.pone.0180243.g001

proteins (7/75), ribosomal and ribosomal biogenesis proteins (9/75), nucleotide-binding proteins potentially implicated in signaling (5/75), energy metabolism (4/75), intracellular trafficking (11/95), carbohydrate metabolism (8/75), mitochondrial function (4/75), and amino acid metabolism (5/75). The remaining proteins were either unclassified or the function was unclear. The first eight groups have a statistical significance of $p < 0.05$, according to the Kyoto Encyclopedia of Genes and Genomes (KEGG) (http://www.kegg.jp/kegg/pathway.html) and search of literature (Fig 3 and S2 Fig). Overall, these findings suggest that Gib2 could modulate a variety of cellular processes and physiological characteristics, some of which are important in the growth and virulence of *C. neoformans*.

Gib2 is involved in ribosomal biogenesis and function

In previous studies, we identified several proteins involved in ribosomal biogenesis and protein translation through GST-Gib2 affinity purification coupled with mass spectrometry [9]. One of these proteins was the eukaryotic initiation factor-4A (eIF4A) homolog that is involved in binding of mRNA to 40S ribosomal subunits (translation initiation) and unwinding of double-stranded RNA (splicing). In that study, we found that the expression of eIF4A was reduced by 3.6- fold in the *gib2* mutant [9]. We also provided structural based evidence pinpointing the interaction between Gib2 and eIF4A [15]. Consistent with these early observations, we found

Spot number	MALDI well number	Match Quality	Top Ranked Protein Name (Species)	Accession No.	Protein MW (Dalton)	Protein PI	Pep.Count	Protein Score	Protein Score C. I. %	Total Ion Score	Total Ion C. I. %	Comments or Other Possibilities
1	C1	-6.03	glyoxal oxidase precursor [Cryptococcus neoformans var. neoformans JEC	gi|58259499	70,760	4.4	6	439	100	426	100	post-translational modification?
2	C2	-3.88	Rds1 protein [Cryptococcus neoformans var. neoformans JEC21]	gi|58262208	41,461	4.4	2	98	100	92	100	post-translational modification?
3	C3	-6.36	glyoxal oxidase precursor [Cryptococcus neoformans var. neoformans JEC	gi|58267754	72,023	4.4	8	159	100	137	100	post-translational modification?
4	C4	-4.48	glyoxal oxidase precursor [Cryptococcus neoformans var. neoformans JEC	gi|58267754	72,023	4.4	8	197	100	175	100	post-translational modification?
5	C5	3.14	heat shock protein [Cryptococcus neoformans var. neoformans JEC21]	gi|58262482	81,914	5.2	9	107	100	86	100	
6	C6	3.27	Conserved oligomeric Golgi complex subunit 6 OS=Cryptococcus neoforma	gi|58258413	83,668	5.3	4	24	0	24	99	
7	C7	2.30	MMS2 [Cryptococcus neoformans var. neoformans JEC21]	gi|58260308	89,401	4.9	10	136	100	108	100	
8	C8	2.38	heat shock protein [Cryptococcus neoformans var. neoformans JEC21]	gi|58261746	85,528	5.1	22	519	100	396	100	post-translational modification?
9	B5	-1.55	FK506-binding protein 1 OS=Cryptococcus neoformans var. grubii GN=FBP	FKBP_CRYNV	11,601	5.7	5	45	98	15	86	post-translational modification?
10	C9	2.90	Plasma membrane fusion protein PRM1 OS=Cryptococcus neoformans var	PRM1_CRYNB	117,304	5.8	6	28	0	28	99	
11	C10	2.35	heat shock protein [Cryptococcus neoformans var. neoformans JEC21]	gi|58258553	99,655	5.9	26	324	100	192	100	
12	C11	3.44	heat shock protein 70 [Cryptococcus neoformans var. neoformans JEC21]	gi|58264706	69,310	4.9	17	189	100	105	100	
13	C12	2.38	heat shock protein [Cryptococcus neoformans var. neoformans JEC21]	gi|58264110	61,260	5.3	32	1300	100	1009	100	
14	C13	2.10	heat shock protein [Cryptococcus neoformans var. neoformans JEC21]	gi|58261136	71,423	5.6	17	417	100	329	100	
15	C14	2.90	heat shock protein [Cryptococcus neoformans var. neoformans JEC21]	gi|58258689	67,086	5.4	26	873	100	673	100	
16	B6	1.94	mitochondrial matrix protein imoo-related protein [Cryptococcus neoforma	gi|58258809	56,846	5.6	9	144	100	113	100	post-translational modification?
17	C15	2.11	pyruvate decarboxylase [Cryptococcus neoformans var. neoformans JEC21	gi|58260130	77,739	6.1	20	567	100	453	100	
18	C16	2.48	pyruvate decarboxylase [Cryptococcus neoformans var. neoformans JEC21	gi|58260130	77,739	6.1	20	552	100	438	100	
19	C17	2.07	pyruvate decarboxylase [Cryptococcus neoformans var. neoformans JEC21	gi|58260130	77,739	6.1	20	590	100	477	100	
20	C18	2.44	proline-tRNA ligase [Cryptococcus neoformans var. neoformans JEC21]	gi|58264302	82,652	5.9	23	563	100	421	100	
21	C19	2.33	3-isopropylmalate dehydratase [Cryptococcus neoformans var. neoformans	gi|58258413	82,816	5.7	18	299	100	209	100	
22	C20	2.45	glycine-tRNA ligase [Cryptococcus neoformans var. neoformans JEC21]	gi|58268176	78,442	6.2	11	267	100	232	100	
23	C21	2.10	5-methyltetrahydropteroyltriglutamate-homocysteine S-methyltransferase [C	gi|58260588	85,308	5.9	17	286	100	208	100	
24	C22	2.10	allantoinase [Cryptococcus neoformans var. neoformans JEC21]	gi|58266478	47,061	4.9	4	156	100	145	100	post-translational modification?
25	C23	2.49	phosphopyruvate hydratase [Cryptococcus neoformans var. neoformans JE	gi|58264446	47,626	5.4	14	649	100	566	100	
26	C24	2.56	hydroxymethylglutaryl-CoA synthase [Cryptococcus neoformans var. neofo	gi|58265298	54,201	5.5	17	514	100	406	100	
27	D1	2.01	hypothetical protein [Cryptococcus neoformans var. neoformans JEC21]	gi|58267444	57,698	5.6	6	166	100	154	100	
28	D2	2.13	glutamate dehydrogenase (NADP+) [Cryptococcus neoformans var. neofor	gi|58264500	49,106	5.9	15	159	100	75	100	
29	D3	2.62	glutamate dehydrogenase (NADP+) [Cryptococcus neoformans var. neofor	gi|58264500	49,106	5.9	14	450	100	368	100	
30	D4	4.31	pyruvate decarboxylase [Cryptococcus neoformans var. neoformans JEC21	gi|58260130	77,739	6.1	9	188	100	163	100	degradation product?
31	D5	2.14	pyruvate decarboxylase [Cryptococcus neoformans var. neoformans JEC21	gi|58260130	77,739	6.1	19	601	100	504	100	degradation product?
32	D6	-2.02	succinate dehydrogenase flavoprotein subunit precursor [Cryptococcus neo	gi|58270950	69,932	6.4	14	488	100	422	100	
33	D7	2.03	hypothetical protein [Cryptococcus neoformans var. neoformans JEC21]	gi|58258193	54,027	6.1	9	146	100	119	100	post-translational modification?
34	B7	-1.58	glutathione disulfide reductase [Cryptococcus neoformans var. neoformans	gi|58267230	52,102	6.2	9	274	100	238	100	
35	B8	1.89	chaperone regulator [Cryptococcus neoformans var. neoformans JEC21]	gi|58263040	44,181	6.0	10	334	100	291	100	post-translational modification?
36	D8	3.35	flavohemoglobin [Cryptococcus neoformans var. grubii]	gi|37783289	55,633	7.0	20	450	100	328	100	see hit #2
37	D9	2.84	flavohemoglobin [Cryptococcus neoformans var. grubii]	gi|37783289	55,633	7.0	20	494	100	373	100	see hit #3
38	D10	2.50	flavohemoglobin [Cryptococcus neoformans var. grubii]	gi|37783289	55,633	7.0	21	465	100	331	100	
39	D11	2.02	flavohemoglobin [Cryptococcus neoformans var. grubii]	gi|37783289	55,633	7.0	20	488	100	366	100	post-translational modification?
40	D12	2.22	sulfide:quinone oxidoreductase mitochondrial precursor [Cryptococcus neof	gi|58260988	49,839	8.9	7	58	98	34	99	
41	D13	-3.53	hypothetical protein CNBE3160 [Cryptococcus neoformans var. neoformans	gi|134112133	48,512	4.6	2	60	99	54	100	
42	D14	-2.04	40S ribosomal protein S0 [Cryptococcus neoformans var. neoformans JEC	gi|58271524	31,450	5.1	7	181	100	147	100	post-translational modification?
43	D15	2.06	L10e protein [Cryptococcus neoformans var. neoformans JEC21]	gi|58269216	33,343	5.2	10	414	100	352	100	
44	D16	2.51	hypothetical protein [Cryptococcus neoformans var. neoformans JEC21]	gi|58267836	43,831	5.8	9	230	100	188	100	
45	D17	3.15	peptidyl-prolyl cis-trans isomerase [Cryptococcus neoformans var. neoform	gi|58268644	40,912	5.8	7	136	100	107	100	post-translational modification?
46	B9	-1.82	allergen [Cryptococcus neoformans var. neoformans JEC21]	gi|58268496	25,832	6.0	5	70	100	44	100	post-translational modification?
47	B10	-1.83	allergen [Cryptococcus neoformans var. neoformans JEC21]	gi|58268496	25,832	6.0	5	367	100	343	100	post-translational modification?
48	D18	-2.45	allergen [Cryptococcus neoformans var. neoformans JEC21]	gi|58268496	25,832	6.0	4	59	99	42	100	post-translational modification?
49	D19	2.17	glyceraldehyde-3-phosphate dehydrogenase [Cryptococcus neoformans va	gi|4761121	36,329	6.3	13	305	100	220	100	
50	D20	2.64	hypothetical protein CNBD4520 [Cryptococcus neoformans var. neoformans	gi|134111162	39,332	9.3	13	298	100	225	100	
51	D21	-2.76	cytochrome-b5 reductase [Cryptococcus neoformans var. neoformans JEC21	gi|58270316	38,387	9.2	11	332	100	270	100	
52	B11	-1.89	wos2 protein (p21) [Cryptococcus neoformans var. neoformans JEC21]	gi|58260772	25,284	4.3	3	191	100	188	100	post-translational modification?
53	B12	-1.65	heat shock protein [Cryptococcus neoformans var. neoformans JEC21]	gi|58258689	67,086	5.4	18	738	100	638	100	degradation product?
54	B13	1.64	hypothetical protein [Cryptococcus neoformans var. neoformans JEC21]	gi|58258843	23,748	5.0	3	81	100	70	100	
55	D22	2.09	h-sco1 [Cryptococcus neoformans var. neoformans JEC21]	gi|58270570	31,678	8.3	12	297	100	213	100	post-translational modification?
56	D23	-4.38	cytoplasm protein [Cryptococcus neoformans var. neoformans JEC21]	gi|58270322	34,431	5.8	20	1210	100	1028	100	
57	D24	-2.11	aconitase [Cryptococcus neoformans var. neoformans JEC21]	gi|58266178	85,959	6.3	10	407	100	379	100	degradation product?
58	E6	2.59	Plasma membrane fusion protein PRM1 OS=Cryptococcus neoformans var	PRM1_CRYNB	117,304	5.8	4	18	0	18	95	degradation product?
59	B14	-1.81	cytoplasm protein [Cryptococcus neoformans var. neoformans JEC21]	gi|58270322	34,431	5.8	14	386	100	288	100	
60	E7	2.10	hypothetical protein [Cryptococcus neoformans var. neoformans JEC21]	gi|58262368	28,410	6.2	5	74	100	53	100	
61	E8	-2.04	zinc-binding dehydrogenase [Cryptococcus neoformans var. neoformans JE	gi|58265458	38,039	5.7	7	84	100	60	100	post-translational modification?
62	B15	-1.73	FK506-binding protein 1 OS=Cryptococcus neoformans var. neoformans se	FKBP_CRYN	11,602	5.7	3	38	90	23	98	post-translational modification?
63	E9	-4.46	allergen [Cryptococcus neoformans var. neoformans JEC21]	gi|58268496	25,832	6.0	3	161	100	151	100	
64	E10	-3.50	allergen [Cryptococcus neoformans var. neoformans JEC21]	gi|58268496	25,832	6.0	6	217	100	188	100	post-translational modification?
65	E11	-3.15	ribulose-phosphate 3-epimerase [Cryptococcus neoformans var. neoformar	gi|58259179	24,179	5.8	7	133	100	94	100	post-translational modification?
66	B16	-1.57	hypothetical protein [Cryptococcus neoformans var. neoformans JEC21]	gi|58258193	54,027	6.1	2	99	100	99	100	degradation product?
67	B17	-1.96	mitochondrial superoxide dismutase Sod2 [Cryptococcus neoformans var. c	gi|57813149	25,899	7.1	9	598	100	538	100	
68	E12	-3.12	mitochondrial superoxide dismutase Sod2 [Cryptococcus neoformans var. c	gi|57813149	25,899	7.1	10	569	100	504	100	
69	E13	-4.01	mitochondrion protein [Cryptococcus neoformans var. neoformans JEC21]	gi|58260552	28,514	8.6	3	89	100	79	100	post-translational modification?
70	B18	1.85	adenylate kinase [Cryptococcus neoformans var. neoformans JEC21]	gi|58261032	29,270	8.8	14	268	100	164	100	
71	B19	-1.97	FK506-binding protein 1 OS=Cryptococcus neoformans var. neoformans se	FKBP_CRYN	11,602	5.7	3	46	98	30	100	post-translational modification?
72	E14	-5.64	hypothetical protein CNA05720 [Cryptococcus neoformans var. neoformans	gi|58258959	18,227	4.6	1	174	100	170	100	post-translational modification?
73	E15	-6.33	60s ribosomal protein l9 [Cryptococcus neoformans var. neoformans JEC21	gi|58258095	21,225	9.2	4	174	100	158	100	post-translational modification?
74	E16	-3.59	translation initiation factor [Cryptococcus neoformans var. neoformans JEC	gi|58259399	45,115	5.1	9	147	100	112	100	degradation product?
75	E17	-6.95	60s ribosomal protein l9 [Cryptococcus neoformans var. neoformans JEC21	gi|58258095	21,225	9.2	4	109	100	92	100	post-translational modification?
76	E18	-2.53	60s ribosomal protein l11 [Cryptococcus neoformans var. neoformans JEC	gi|58260012	19,770	10.3	6	82	100	52	100	post-translational modification?
77	E19	2.45	hypothetical protein [Cryptococcus neoformans var. neoformans JEC21]	gi|58270280	18,634	5.2	7	176	100	128	100	
78	E20	2.48	FK506-binding protein 1 OS=Cryptococcus neoformans var. neoformans se	FKBP_CRYN	11,602	5.7	3	38	87	22	97	post-translational modification?
79	E21	-4.22	allergen [Cryptococcus neoformans var. neoformans JEC21]	gi|58268496	25,832	6.0	2	123	100	116	100	
80	E22	-3.21	inorganic diphosphatase [Cryptococcus neoformans var. neoformans JEC2	gi|58267854	35,293	6.1	6	61	99	38	99	degradation product?
81	E23	2.23	40s ribosomal protein s5-1 [Cryptococcus neoformans var. neoformans JEC	gi|58261010	22,659	9.7	8	255	100	208	100	post-translational modification?
82	E24	-3.35	hypothetical protein [Cryptococcus neoformans var. neoformans JEC21]	gi|58271446	11,860	4.6	6	585	100	535	100	
83	F1	-3.89	histone h2b [Cryptococcus neoformans var. neoformans JEC21]	gi|58263312	14,744	10.2	5	61	99	36	99	post-translational modification?
84	F2	-3.26	ribosomal protein [Cryptococcus neoformans var. neoformans JEC21]	gi|58260222	15,423	10.6	8	194	100	140	100	post-translational modification?
85	F3	-2.66	ribosomal protein 22 of the small subunit [Cryptococcus neoformans var. ne	gi|58260950	14,431	10.2	2	185	100	176	100	post-translational modification?
86	B20	-1.69	ribosomal protein [Cryptococcus neoformans var. neoformans JEC21]	gi|58260222	15,423	10.6	6	84	100	49	100	post-translational modification?
87	B21	-1.58	40S ribosomal protein S12 [Cryptococcus neoformans var. neoformans JEC	gi|58264912	15,936	5.0	4	97	100	75	100	
88	B22	-1.66	FK506-binding protein 1 OS=Cryptococcus neoformans var. neoformans se	FKBP_CRYN	11,602	5.7	4	45	98	22	98	post-translational modification?
89	B23	-1.65	Hmp1 protein [Cryptococcus neoformans var. neoformans JEC21]	gi|58264506	11,779	5.3	2	88	100	78	100	
90	B24	-1.55	cytochrome c oxidase polypeptide IV mitochondrial precursor [Cryptococcu	gi|58261242	22,912	6.2	4	589	100	569	100	degradation product?
91	C1	1.75	hypothetical protein CNM00840 [Cryptococcus neoformans var. neoformans	gi|58262020	14,841	6.3	7	587	100	530	100	
92	C2	1.84	FK506-binding protein 1 OS=Cryptococcus neoformans var. neoformans se	FKBP_CRYN	11,602	5.7	4	44	97	21	97	
93	C3	-1.55	hypothetical protein CNBE4310 [Cryptococcus neoformans var. neoformans	gi|134113454	9,148	5.8	4	108	100	77	100	post-translational modification?
94	F4	-2.53	cytochrome c oxidase subunit V [Cryptococcus neoformans var. neoformans	gi|58260682	18,283	9.3	7	422	100	372	100	post-translational modification?

Fig 2. Identification of differentially expressed proteins due to *GIB2* gene disruption by MALDI-TOF-TOF MS analysis. Proteins were digested with trypsin overnight and processed protein samples were analyzed by LC-electrospray ionization-MS/MS using a Finnigan LTQ ion trap mass spectrometer [9]. The acquired raw data were processed using BioWorks (version 3.3) (Thermo Electron).

https://doi.org/10.1371/journal.pone.0180243.g002

that a large number of differentially expressed proteins were either ribosomal components or proteins associated with ribosomal function (Fig 2). The abundance of ribosomal and ribosomal biogenesis associated proteins (11) was remarkably changed in the *gib2* mutant, in comparison to that in the wild type H99 strain. Among these proteins, nine were decreased in expression, and only two (gi 58261010 and gi 58269216) were increased (Fig 2). Among those decreased, the putative 60S ribosomal protein L9 (gi 58258095) appears to be the most affected with reductions of 6.3- to 7- fold.

To investigate if the changes in protein expression were rather due to mRNA abundance changes than modulated protein translation, we opted to use the semi-quantitative RT-PCR approach to examine the expression of four selected genes that correspond to proteins with the most changes. The Hsp70-like protein (spot 12, gi 5826470) and flavohemoglobin (spot 36, gi 37783289) were increased by at least 3 folds in the *gib2* mutant, whereas the glyoxal oxidase precursor (spot 3, gi 58267754) and 60S ribosomal protein L9 (spot 75, gi 58258095) were decreased in expression by at least 6- folds. However, as revealed by semi-quantitative RT-PCR analysis, the expression of these genes was largely similar between both strains. Relative abundance of Hsp70, flavohemoglobin, glyoxal precursor, and 60S ribosome L9 are 2.0± 0.2, 1.7±0.1, 2.2±0.4, and 2.3±0.2 in H99 versus 2.3±0.4, 1.6±0.3, 2.1±0.2, and 2±0.2 in the *Gib2* mutant (Fig 4). Collectively, these findings suggest that Gib2 participates in ribosomal biogenesis and protein translation.

Gib2 has roles in stress responses

The 70-kilo Dalton heat shock proteins (Hsp70 or DnaK) are a family of highly conserved, ubiquitously expressed proteins that chaperone the folding of a large variety of proteins. Hsp70 proteins also help to protect cells from the stress caused by hyperthermia, oxidants, or changes in pH (reviewed in [24,25]). Our DIGE data indicated that *C. neoformans* could encode at least six Hsp70 and one Hsp71 protein homologs, whose translation are all subject to regulation by Gib2. Indeed, all these proteins were increased in abundance by 2.1- to 3.4-fold. The expression of Ssa1, one of the Hsp70 proteins containing a DEAD domain and is involved in the stress response [26,27] was mostly increased by 3.4- fold. Given the established roles of Hsp70 proteins, the increased expression of Hsp70/71 proteins may functionally compensate for a lack of Gib2 adaptor/ chaperon function needed for nascent protein synthesis, folding, and maturation.

Gib2 has roles in intracellular trafficking

In a previous study, we found that Gib2 interacts with Cin1, a homolog of human intersectin ITSN1 protein, in *C. neoformans* [10]. The Cin1 protein shares a high amino acid sequence homology with the mammalian intersectin ITSN1 protein [28]. We subsequently demonstrated Cin1 as an endocytic adaptor protein that has a pleiotropic function important for endocytosis, actin cytoskeleton dynamics, and virulence [29]. The current 2-DIGE study results support the involvement of Gib2 in Cin1-regulated intracellular trafficking. Indeed, as indicated by our current findings, the expression of eight putative intracellular trafficking proteins was differentially affected due to the *GIB2* gene disruption. As shown in Fig 2, the expression of plasma fusion protein Prm1 OS (Prm1_Crynb) showed a 2.6- fold of increase in the

Functional Group 1	Enrichment Score: 5.8763947895872155								
Category	Term	Count	%	PValue	Genes	List Total	Fold Enrichment	Bonferroni	FDR
INTERPRO	IPR018181:Heat shock protein 70, conserved site	5	7.936507937	8.97E-07	58261136, 58264706, 58262482, 58261746, 58258689	56	61.69642857	1.38E-04	0.00107645
INTERPRO	IPR001023:Heat shock protein Hsp70	5	7.936507937	1.62E-06	58261136, 58264706, 58262482, 58261746, 58258689	56	53.984375	2.49E-04	0.00194071
INTERPRO	IPR013126:Heat shock protein 70	5	7.936507937	1.62E-06	58261136, 58264706, 58262482, 58261746, 58258689	56	53.984375	2.49E-04	0.00194071
Functional Group 2	**Enrichment Score: 3.310504678405634**								
Category	Term	Count	%	PValue	Genes	List Total	Fold Enrichment	Bonferroni	FDR
KEGG_PATHWAY	cne03010:Ribosome	8	12.6984127	5.36E-05	58271524, 58264912, 58258095, 58260012, 58261010	29	7.274977895	0.001178353	0.04193516
SP_PIR_KEYWORDS	ribosomal protein	8	12.6984127	5.41E-05	58271524, 58264912, 58258095, 58260012, 58261010	60	7.949019603	0.002699123	0.0520495
GOTERM_MF_FAT	GO:0003735~structural constituent of ribosome	8	12.6984127	0.001974131	58271524, 58264912, 58258095, 58260012, 58261010	47	4.306812087	0.207987492	2.2361275
GOTERM_MF_FAT	GO:0005198~structural molecule activity	8	12.6984127	0.010015671	58271524, 58264912, 58258095, 58260012, 58261010	47	3.203191489	0.695109141	10.8812520
Functional Group 3	**Enrichment Score: 2.249578916981557**								
Category	Term	Count	%	PValue	Genes	List Total	Fold Enrichment	Bonferroni	FDR
GOTERM_CC_FAT	GO:0005740~mitochondrial envelope	9	14.28571429	0.001725555	58261136, 58261032, 58265188, 58270950, 58260682	35	3.724175824	0.116927112	1.78158376
GOTERM_CC_FAT	GO:0031967~organelle envelope	9	14.28571429	0.009792405	58261136, 58261032, 58265188, 58270950, 58260682	35	2.811152074	0.507631479	9.73579188
GOTERM_CC_FAT	GO:0031975~envelope	9	14.28571429	0.010554657	58261136, 58261032, 58265188, 58270950, 58260682	35	2.775341219	0.534188572	10.456430
Functional Group 4	**Enrichment Score: 2.0154916290278475**								
Category	Term	Count	%	PValue	Genes	List Total	Fold Enrichment	Bonferroni	FDR
GOTERM_BP_FAT	GO:0006626~protein targeting to mitochondrion	4	6.349206349	0.004038495	58261136, 58264110, 58258809, 58263040	46	12.02120891	0.589454307	5.02074579
GOTERM_BP_FAT	GO:0070585~protein localization in mitochondrion	4	6.349206349	0.004038495	58261136, 58264110, 58258809, 58263040	46	12.02120891	0.589454307	5.02074579
GOTERM_BP_FAT	GO:0006839~mitochondrial transport	4	6.349206349	0.005942845	58261136, 58264110, 58258809, 58263040	46	10.48658649	0.730537725	7.30674995
GOTERM_BP_FAT	GO:0007005~mitochondrion organization	4	6.349206349	0.028504365	58261136, 58264110, 58258809, 58263040	46	5.867494824	0.998274211	30.7962432
GOTERM_BP_FAT	GO:0017038~protein import	4	6.349206349	0.030282835	58261136, 58264110, 58258809, 58263040	46	5.731041455	0.998846763	32.3917017
Functional Group 5	**Enrichment Score: 1.78599569521563**								
Category	Term	Count	%	PValue	Genes	List Total	Fold Enrichment	Bonferroni	FDR
GOTERM_CC_FAT	GO:0045277~respiratory chain complex IV	3	4.761904762	0.001988345	58265188, 58260682, 58261242	35	41.49795918	0.133509039	2.05037365
GOTERM_CC_FAT	GO:0005751~mitochondrial respiratory chain complex IV	3	4.761904762	0.001988345	58265188, 58260682, 58261242	35	41.49795918	0.133509039	2.05037365
GOTERM_MF_FAT	GO:0016676~oxidoreductase activity, acting on heme group of donors	3	4.761904762	0.008080465	58265188, 58260682, 58261242	47	21.35460993	0.616098251	8.86713019
GOTERM_MF_FAT	GO:0016675~oxidoreductase activity, acting on heme group of donors	3	4.761904762	0.008080465	58265188, 58260682, 58261242	47	21.35460993	0.616098251	8.86713019
GOTERM_MF_FAT	GO:0015002~heme-copper terminal oxidase activity	3	4.761904762	0.008080465	58265188, 58260682, 58261242	47	21.35460993	0.616098251	8.86713019
GOTERM_MF_FAT	GO:0004129~cytochrome-c oxidase activity	3	4.761904762	0.008080465	58265188, 58260682, 58261242	47	21.35460993	0.616098251	8.86713019
GOTERM_MF_FAT	GO:0015078~hydrogen ion transmembrane transporter activity	3	4.761904762	0.134448505	58265188, 58260682, 58261242	47	4.575987842	0.99999993	80.8417395
GOTERM_MF_FAT	GO:0015077~monovalent inorganic cation transmembrane transporter activity	3	4.761904762	0.142275565	58265188, 58260682, 58261242	47	4.418195153	0.999999983	82.7334131
GOTERM_MF_FAT	GO:0022890~inorganic cation transmembrane transporter activity	3	4.761904762	0.261589983	58265188, 58260682, 58261242	47	2.956792144	1	96.8900954
Functional Group 6	**Enrichment Score: 1.6013130517702017**								
Category	Term	Count	%	PValue	Genes	List Total	Fold Enrichment	Bonferroni	FDR
GOTERM_BP_FAT	GO:0015031~protein transport	8	12.6984127	0.023874157	58261136, 58264110, 58264706, 58262482, 58260308	46	2.693276313	0.995087776	26.4783382
GOTERM_BP_FAT	GO:0045184~establishment of protein localization	8	12.6984127	0.023874157	58261136, 58264110, 58264706, 58262482, 58260308	46	2.693276313	0.995087776	26.4783382
GOTERM_BP_FAT	GO:0008104~protein localization	8	12.6984127	0.027555265	58261136, 58264110, 58264706, 58262482, 58260308	46	2.614692654	0.997860639	29.9306837
Functional Group 7	**Enrichment Score: 1.526169872526088**								
Category	Term	Count	%	PValue	Genes	List Total	Fold Enrichment	Bonferroni	FDR
GOTERM_BP_FAT	GO:0033365~protein localization in organelle	6	9.523809524	0.001792537	58261136, 58264110, 58264706, 58262482, 58258809	46	6.600931677	0.326125987	2.25795691
GOTERM_BP_FAT	GO:0006605~protein targeting	6	9.523809524	0.008925725	58261136, 58264110, 58264706, 58262482, 58258809	46	4.535609493	0.86088803	10.7857325
GOTERM_BP_FAT	GO:0006886~intracellular protein transport	6	9.523809524	0.050678995	58261136, 58264110, 58264706, 58262482, 58258809	46	2.887907609	0.999989263	48.4198820
GOTERM_BP_FAT	GO:0034613~cellular protein localization	6	9.523809524	0.057243365	58261136, 58264110, 58264706, 58262482, 58258809	46	2.789827723	0.999997667	52.7803894
GOTERM_BP_FAT	GO:0070727~cellular macromolecule localization	6	9.523809524	0.060313627	58261136, 58264110, 58264706, 58262482, 58258809	46	2.748343	0.999998862	54.7009543
GOTERM_BP_FAT	GO:0046907~intracellular transport	6	9.523809524	0.248828625	58261136, 58264110, 58264706, 58262482, 58258809	46	1.731391915	1	97.380411
Functional Group 8	**Enrichment Score: 1.2388579869104204**								
Category	Term	Count	%	PValue	Genes	List Total	Fold Enrichment	Bonferroni	FDR
GOTERM_MF_FAT	GO:0030554~adenyl nucleotide binding	14	22.22222222	0.029349835	58261136, 58270950, 58261746, 58268176, 58258689	47	1.819256833	0.970255804	28.8883202
GOTERM_MF_FAT	GO:0001883~purine nucleoside binding	14	22.22222222	0.029349835	58261136, 58270950, 58261746, 58268176, 58258689	47	1.819256833	0.970255804	28.8883202
GOTERM_MF_FAT	GO:0001882~nucleoside binding	14	22.22222222	0.031625065	58261136, 58270950, 58261746, 58268176, 58258689	47	1.800991199	0.977450451	30.7727721
GOTERM_MF_FAT	GO:0017076~purine nucleotide binding	14	22.22222222	0.085168005	58261136, 58270950, 58261746, 58268176, 58258689	47	1.559814983	0.999972567	63.8943165
GOTERM_MF_FAT	GO:0000166~nucleotide binding	14	22.22222222	0.275543884	58261136, 58270950, 58261746, 58268176, 58258689	47	1.263230447	1	97.500088
Functional Group 9	**Enrichment Score: 0.9626019110470618**								
Category	Term	Count	%	PValue	Genes	List Total	Fold Enrichment	Bonferroni	FDR
GOTERM_MF_FAT	GO:0005524~ATP binding	12	19.04761905	0.068030065	58261136, 58258553, 58264110, 58264706, 58261032	47	1.725625045	0.999754854	55.3497752
GOTERM_MF_FAT	GO:0032559~adenyl ribonucleotide binding	12	19.04761905	0.070302705	58261136, 58258553, 58264110, 58264706, 58261032	47	1.715995441	0.999816217	56.580104
GOTERM_MF_FAT	GO:0032553~ribonucleotide binding	12	19.04761905	0.171774905	58261136, 58258553, 58264110, 58264706, 58261032	47	1.453243773	1	88.4319867
GOTERM_MF_FAT	GO:0032555~purine ribonucleotide binding	12	19.04761905	0.171774905	58261136, 58258553, 58264110, 58264706, 58261032	47	1.453243773	1	88.4319867
Functional Group 10	**Enrichment Score: 0.8459001590835294**								
Category	Term	Count	%	PValue	Genes	List Total	Fold Enrichment	Bonferroni	FDR
GOTERM_BP_FAT	GO:0042257~ribosomal subunit assembly	3	4.761904762	0.039725447	58271524, 58260012, 58269216	46	9.241304343	0.999860035	40.3096166
GOTERM_BP_FAT	GO:0042255~ribosome assembly	3	4.761904762	0.059370945	58271524, 58260012, 58269216	46	7.393043473	0.999998581	54.1190708
GOTERM_BP_FAT	GO:0022618~ribonucleoprotein complex assembly	3	4.761904762	0.079324805	58271524, 58260012, 58269216	46	6.265291083	0.999999987	65.0781907
GOTERM_BP_FAT	GO:0042254~ribosome biogenesis	3	4.761904762	0.550841277	58271524, 58260012, 58269216	46	1.607183365	1	99.9962393
GOTERM_BP_FAT	GO:0022613~ribonucleoprotein complex biogenesis	3	4.761904762	0.572032825	58271524, 58260012, 58269216	46	1.546661815	1	99.9979672
Functional Group 11	**Enrichment Score: 0.8177999448494516**								
Category	Term	Count	%	PValue	Genes	List Total	Fold Enrichment	Bonferroni	FDR
GOTERM_BP_FAT	GO:0006007~glucose catabolic process	3	4.761904762	0.101049435	58260130, 58259179, 58264446	46	5.436061381	1	74.2317520
GOTERM_BP_FAT	GO:0019320~hexose catabolic process	3	4.761904762	0.101049435	58260130, 58259179, 58264446	46	5.436061381	1	74.2317520
GOTERM_BP_FAT	GO:0046365~monosaccharide catabolic process	3	4.761904762	0.106083795	58260130, 58259179, 58264446	46	5.280745342	1	76.0095788
GOTERM_BP_FAT	GO:0046164~alcohol catabolic process	3	4.761904762	0.140314875	58260130, 58259179, 58264446	46	4.45364065	1	85.4057936
GOTERM_BP_FAT	GO:0044275~cellular carbohydrate catabolic process	3	4.761904762	0.16243745	58260130, 58259179, 58264446	46	4.062111801	1	89.5273650
GOTERM_BP_FAT	GO:0006006~glucose metabolic process	3	4.761904762	0.182288895	58260130, 58259179, 58264446	46	3.771960953	1	92.2829800
GOTERM_BP_FAT	GO:0016052~carbohydrate catabolic process	3	4.761904762	0.225894335	58260130, 58259179, 58264446	46	3.271258173	1	96.158556
GOTERM_BP_FAT	GO:0019318~hexose metabolic process	3	4.761904762	0.282116225	58260130, 58259179, 58264446	46	2.800395257	1	98.5288518
Functional Group 12	**Enrichment Score: 0.6201505414002227**								
Category	Term	Count	%	PValue	Genes	List Total	Fold Enrichment	Bonferroni	FDR
GOTERM_BP_FAT	GO:0008652~cellular amino acid biosynthetic process	4	6.349206349	0.147697355	58258413, 58264500, 58260588, 58266178	46	2.933747412	1	86.9231969
GOTERM_BP_FAT	GO:0009309~amine biosynthetic process	4	6.349206349	0.162900095	58258413, 58264500, 58260588, 58266178	46	2.800395257	1	89.6007574
GOTERM_BP_FAT	GO:0016053~organic acid biosynthetic process	4	6.349206349	0.229946275	58258413, 58264500, 58260588, 58266178	46	2.358227585	1	96.4067999
GOTERM_BP_FAT	GO:0046394~carboxylic acid biosynthetic process	4	6.349206349	0.229946275	58258413, 58264500, 58260588, 58266178	46	2.358227585	1	96.4067999
Functional Group 2	**Enrichment Score: 5.8763947895872155**								

Fig 3. Functional groups of differentially expressed proteins due to *GIB2* disruption. The grouping was based on KEGG (http://www.kegg.jp/kegg/pathway.html) and a search of the literature (see Materials and Methods). Following protein identification, pathway analysis and protein clustering were performed using the Database for Annotation, Visualization, and Integrated Discovery (DAVID, NIAID/NIH).

https://doi.org/10.1371/journal.pone.0180243.g003

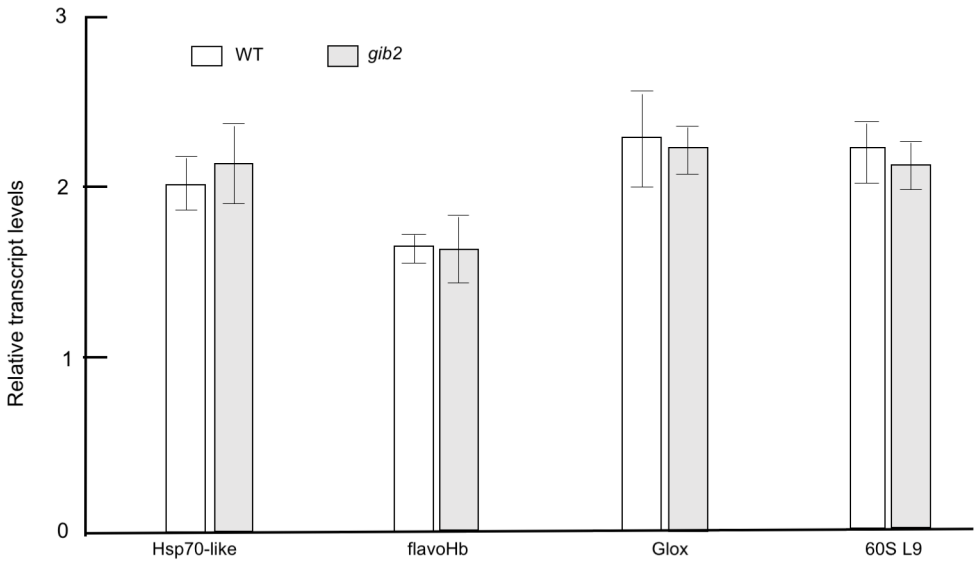

Fig 4. Differences in expressions of four representative genes are largely similar between the wild type and the *gib2* mutant strains. The induction time for cells in YNB was 3 hours. RT-PCR was repeated twice and mean values were used to calculate the expression rate relative to that of the *ACT* gene encoding actin with error bars (average + SD) shown. PCR cycles were limited to 25. Hsp70-like, flavoHb, Glox, and 60S L9 denote, respectively, a Hsp70 protein homolog (spot 12, gi 5826470), flavohemoglobin (spot 36, gi 37783289), a glyoxal oxidase precursor (spot 3, gi 58267754), and 60S ribosomal protein L9 (spot 75, gi 58258095).

https://doi.org/10.1371/journal.pone.0180243.g004

gib2 mutant strain. Similarly, the expression of a conserved oligomeric Golgi complex subunit 6 (Cog6_Crynj) putatively involved in ER to Golgi vesicle transport was increased by 3.3- fold because of *GIB2* gene disruption (Fig 2).

Discussion

The human fungal pathogen *Cryptococcus neoformans* remains a significant cause of morbidity and mortality in individuals with compromised immune status, especially in regions of high HIV prevalence and limited healthcare resources [30]. Upon inhalation, the fungus exhibits a predilection for the human central nervous system where it can cause potentially fatal meningoencephalitis if untreated. Virulence of the fungus is a multifaceted and attributable to multiple and diverse traits. Among those of pathogenic-intrinsic origin, signal transduction pathways are means by which the fungus senses and responds to environmental stimuli and produces virulence factors. In *C. neoformans*, Gpa1- and Gpb1-mediated G-protein signal transduction pathways, as well as additional signaling molecules or pathways, are important in the modulation of growth and pathogenesis (reviewed in [2,31]).

Our previous studies established that Gib2 participates in Gpa1 signaling as an atypical Gβ-like protein through coupling with Gpa1 and Gpg1/Gpg2 as a heterotrimeric complex, and Gib2 also positively promotes cAMP signaling independent of Gpa1 [10]. These studies demonstrated that Gib2 is a critical component of overall signal transduction pathways required for normal growth and virulence of *C. neoformans*. Importantly, Gib2 interacts with at least 47 additional proteins with diverse functions, indicating its capacity as a regulatory scaffold protein to modulate multiple protein-protein interactions, similar to Gβ-like/RACK1/Asc1 family proteins of other organisms. To examine this multifaceted role at the genome-wide level, we performed a protein expression profiling study by 2D-DIGE coupled with mass spectrometry

analysis. Using pathway analysis of predicted proteins identified in the Protein ID report, we clustered 76 proteins into 12 functional protein groups. Among the groups, ribosomal subunits, ribosomal biogenesis components, intracellular trafficking, and signaling components are included in the top of the eight groups. Together with our previous findings, this new round of findings further established crucial function of Gib2 in growth and pathogenicity [9]. Significantly, these findings also suggest that Gib2 represents an important therapeutic target.

Our finding is highly accordant with those of human and *S. cerevisiae* studies indicating Gβ-like/RACK1 and Asc1 proteins are ribosomal core proteins [10,11,12,13,14,15]. In these studies, Gβ-like/RACK1 and Asc1 were found to interact with the 40S ribosome subunit largely via the RDK (Arg36-Asp37-Lys38) amino acid residues in the first WD40 domain. Moreover, Gβ-like/RACK and Asc1 associate with the head region of the 40S ribosomal subunit in the vicinity of the mRNA exit channel [32,33]. Gib2 also contains the exact RDK residues in its sequence [9]. LACK1, a RACK/Asc1/Gib2 homolog in the parasite *Leishmania major* contains the conserved RDK/G residues and was located in the polysome (polyribosome) complex [34]. In addition, the eukaryotic initiation factor 4A (eIF4A) is required for the binding of mRNA to 40S ribosomal subunits (translation initiation) and unwinding double-stranded RNA (splicing). In *Leishmania*, the parasite cells deficient in LACK were more susceptible to hippuristanol, an eIF4A-specific inhibitor, than WT control strains [34]. Using GST-tagged protein purification and co-immunoprecipitation approaches, we earlier demonstrated that Gib2 interact with eIF4A [9]. We further mapped out the Gib2-eIF4A interaction based on the analysis of the Gib2 crystal structure [15]. Although not demonstrated in this study, the expression of eIF4A was reduced by 3.6- fold in the *gib2* mutant, supporting that Gib2 has a significant role in the initiation of protein translation.

Eukaryotic Hsp70/71 proteins are involved in the modulation of nascent protein folding and processing, thereby protecting cells from the stress. The findings that Gib2 exerts a strong influence over the expression of all Hsp70/71 homologs may suggest their elevated expression is a compensatory effect made by in the *gib2* mutant cells (or that loss of Gib2 induces cellular stress). Overexpression of Hsp70/71 proteins may compensate for the lack of Gib2 in protein translation. One of the resulting functions of increased Hsp70 proteins is that they provide a means of protection against stresses, whether it is hyperthermia, the oxidative stress, or host-mediated stress conditions.

Finally, given the importance of Gib2 in modulating signaling pathways, we failed to identify relevant proteins in DIGE coupled with mass spectrometry. We hypothesized that this may be due to the nature of regulatory proteins whose expressions may be highly regulated either spatially or temporally and that our sampling method failed to meet these specific conditions. Nevertheless, by employing the genome-wide global approach, we gained further insights into the complex function and pathway of Gib2 biology that is important for morphogenesis, development, and pathogenicity. Significantly, this approach has allowed for the simultaneous examination of multiple proteins subjected to translational regulation by Gib2. Further examination of these proteins and the pathways they represent are likely to expose more potential targets for therapeutic intervention of infection caused by *C. neoformans*.

Supporting information

S1 Fig. Primers used in this study.
(TIFF)

S2 Fig. MALDI-TOF-TOF MS analysis of differentially expressed proteins in *C. neoformans*.
(XLS)

Acknowledgments

We thank Kelly, Zhang, and Wang lab members for their helps and anonymous reviewers for their helpful suggestions.

Author Contributions

Conceptualization: GOB ZGZ PW.

Data curation: GOB BK ZGZ PW.

Formal analysis: GOB BB BK ZGZ PW.

Funding acquisition: ZGZ PW.

Investigation: GOB BK ZGZ PW.

Methodology: GOB BB BK ZGZ PW.

Project administration: PW.

Resources: BK ZGZ PW.

References

1. Casadevall A, Perfect JR (1998) Cryptococcus neoformans. Washington: ASM Press. 1–541 p.
2. Wang P, Fox DS (2005) *Cryptococcus neoformans* evolves as a model of choice for studying signaling transduction. In: Xu JP, editor. Evolutionary Genetics of Fungi. Norfolk, UK: Horizon Bioscience. pp. 321–338.
3. Li L, Shen G, Zhang ZG, Wang YL, Thompson JK, and Wang P. (2007) Canonical heterotrimeric G proteins regulating mating and virulence of *Cryptococcus neoformans*. Mol Biol Cell 18: 4201–4209. https://doi.org/10.1091/mbc.E07-02-0136 PMID: 17699592
4. Alspaugh JA, Pukkila-Worley R, Harashima T, Cavallo LM, Funnell D, Cox GM, et al. (2002) Adenylyl cyclase functions downstream of the Galpha protein Gpa1 and controls mating and pathogenicity of *Cryptococcus neoformans*. Eukaryot Cell 1: 75–84. https://doi.org/10.1128/EC.1.1.75-84.2002 PMID: 12455973
5. Davidson RC, Blankenship JR, Kraus PR, de Jesus Berrios M, Hull CM, Wang P, et al. (2002) A PCR-based strategy to generate integrative targeting alleles with large regions of homology. Microbiology 148: 2607–2615. https://doi.org/10.1099/00221287-148-8-2607 PMID: 12177355
6. Bahn YS, Hicks JK, Giles SS, Cox GM, Heitman J (2004) Adenylyl cyclase-associated protein Aca1 regulates virulence and differentiation of *Cryptococcus neoformans* via the cyclic AMP-protein kinase A cascade. Eukaryot Cell 3: 1476–1491. https://doi.org/10.1128/EC.3.6.1476-1491.2004 PMID: 15590822
7. Wang P, Heitman J (1999) Signal transduction cascades regulating mating, filamentation, and virulence in *Cryptococcus neoformans*. Curr Opinion Microbiol 2: 358–362.
8. Hsueh YP, Xue C, Heitman J (2007) G protein signaling governing cell fate decisions involves opposing Galpha subunits in *Cryptococcus neoformans*. Mol Biol Cell 18: 3237–3249. https://doi.org/10.1091/mbc.E07-02-0133 PMID: 17581859
9. Wang Y, Shen G, Gong J, Shen D, Whittington A, Qing J, et al. (2014) Noncanonical Gbeta Gib2 is a scaffolding protein promoting cAMP signaling through functions of Ras1 and Cac1 in *Cryptococcus neoformans*. J Biol Chem 289: 12202–12216. https://doi.org/10.1074/jbc.M113.537183 PMID: 24659785
10. Palmer DA, Thompson JK, Li L, Prat A, Wang P (2006) Gib2, a novel Gbeta-like/RACK1 homolog, functions as a Gbeta subunit in cAMP signaling and is essential in *Cryptococcus neoformans*. J Biol Chem 281: 32596–32605. https://doi.org/10.1074/jbc.M602768200 PMID: 16950773
11. Gerbasi VR, Weaver CM, Hill S, Friedman DB, Link AJ (2004) Yeast Asc1p and mammalian RACK1 are functionally orthologous core 40S ribosomal proteins that repress gene expression. Mol Cell Biol 24: 8276–8287. https://doi.org/10.1128/MCB.24.18.8276-8287.2004 PMID: 15340087
12. Valerius O, Kleinschmidt M, Rachfall N, Schulze F, Lopez Marin S, Hoppert M, et al. (2007) The *Saccharomyces* homolog of mammalian RACK1, Cpc2/Asc1p, is required for FLO11-dependent adhesive

growth and dimorphism. Mol Cell Proteomics 6: 1968–1979. https://doi.org/10.1074/mcp.M700184-MCP200 PMID: 17704055

13. Ceci M, Gaviraghi C, Gorrini C, Sala LA, Offenhauser N, Marchisio PC, et al. (2003) Release of eIF6 (p27BBP) from the 60S subunit allows 80S ribosome assembly. Nature 426: 579–584. https://doi.org/10.1038/nature02160 PMID: 14654845
14. Nilsson J, Sengupta J, Frank J, Nissen P (2004) Regulation of eukaryotic translation by the RACK1 protein: a platform for signalling molecules on the ribosome. EMBO Rep 5: 1137–1141. https://doi.org/10.1038/sj.embor.7400291 PMID: 15577927
15. Ero R, Dimitrova VT, Chen Y, Bu W, Feng S, Liu TB, et al. (2015) Crystal structure of Gib2, a signal-transducing protein scaffold associated with ribosomes in *Cryptococcus neoformans*. Sci Rep 5: 8688. https://doi.org/10.1038/srep08688 PMID: 25732347
16. Kim YN, Kim HK, Warda M, Kim N, Park WS, Price AB, et al. (2007) Toward a better understanding of preeclampsia: Comparative proteomic analysis of preeclamptic placentas. Proteomics Clinical applications 1: 1625–1636. https://doi.org/10.1002/prca.200700034 PMID: 21136660
17. Doyle S (2011) Fungal proteomics: from identification to function. FEMS microbiology letters 321: 1–9. https://doi.org/10.1111/j.1574-6968.2011.02292.x PMID: 21517945
18. O'Farrell PH (1975) High resolution two-dimensional electrophoresis of proteins. The Journal of biological chemistry 250: 4007–4021. PMID: 236308
19. Unlu M, Morgan ME, Minden JS (1997) Difference gel electrophoresis: a single gel method for detecting changes in protein extracts. Electrophoresis 18: 2071–2077. https://doi.org/10.1002/elps.1150181133 PMID: 9420172
20. Alban A, David SO, Bjorkesten L, Andersson C, Sloge E, Lewis S, et al. (2003) A novel experimental design for comparative two-dimensional gel analysis: two-dimensional difference gel electrophoresis incorporating a pooled internal standard. Proteomics 3: 36–44. https://doi.org/10.1002/pmic.200390006 PMID: 12548632
21. Perfect JR, Lang SDR, Durack DT (1980) Chronic cryptococcal meningitis: a new experimental model in rabbits. Am J Pathol 101: 177–194. PMID: 7004196
22. Bradford MM (1976) A rapid and sensitive method for the quantitation of microgram quantities of protein utilizing the principle of protein-dye binding. Analytical biochemistry 72: 248–254. PMID: 942051
23. Gong J, Grodsky JD, Zhang Z, Wang P (2014) A Ric8/synembryn homolog promotes Gpa1 and Gpa2 activation to respectively regulate cyclic AMP and pheromone signaling in *Cryptococcus neoformans*. Eukaryot Cell 13: 1290–1299. https://doi.org/10.1128/EC.00109-14 PMID: 25084863
24. Mayer MP, Bukau B (2005) Hsp70 chaperones: cellular functions and molecular mechanism. Cellular and molecular life sciences: CMLS 62: 670–684. https://doi.org/10.1007/s00018-004-4464-6 PMID: 15770419
25. Sharma D, Masison DC (2009) Hsp70 structure, function, regulation and influence on yeast prions. Protein and peptide letters 16: 571–581. PMID: 19519514
26. Zhang S, Hacham M, Panepinto J, Hu G, Shin S, Zhu X, et al. (2006) The Hsp70 member, Ssa1, acts as a DNA-binding transcriptional co-activator of laccase in *Cryptococcus neoformans*. Mol Microbiol 62: 1090–1101. https://doi.org/10.1111/j.1365-2958.2006.05422.x PMID: 17040492
27. Eastman AJ, He X, Qiu Y, Davis MJ, Vedula P, Lyons DM, et al. (2015) Cryptococcal heat shock protein 70 homolog Ssa1 contributes to pulmonary expansion of *Cryptococcus neoformans* during the afferent phase of the immune response by promoting macrophage M2 polarization. Journal of immunology 194: 5999–6010.
28. Wong KA, Wilson J, Russo A, Wang L, Okur MN, Wang XR, et al. (2012) Intersectin (ITSN) family of scaffolds function as molecular hubs in protein interaction networks. PLoS One 7: e36023. https://doi.org/10.1371/journal.pone.0036023 PMID: 22558309
29. Shen G, Whittington A, Song K, Wang P (2010) Pleiotropic function of intersectin homologue Cin1 in *Cryptococcus neoformans*. Mol Microbiol 76: 662–676. https://doi.org/10.1111/j.1365-2958.2010.07121.x PMID: 20345666
30. Park BJ, Wannemuehler KA, Marston BJ, Govender N, Pappas PG, Chiller TM. (2009) Estimation of the current global burden of cryptococcal meningitis among persons living with HIV/AIDS. AIDS 23: 525–530. https://doi.org/10.1097/QAD.0b013e328322ffac PMID: 19182676
31. Lengeler KB, Davidson RC, D'Souza C, Harashima T, Shen W-C, et al. (2000) Signal transduction cascades regulating fungal development and virulence. Microbiol Mol Biol Rev 64: 746–785. PMID: 11104818
32. Coyle SM, Gilbert WV, Doudna JA (2009) Direct link between RACK1 function and localization at the ribosome in vivo. Mol Cell Biol 29: 1626–1634. https://doi.org/10.1128/MCB.01718-08 PMID: 19114558

33. Rabl J, Leibundgut M, Ataide SF, Haag A, Ban N (2011) Crystal structure of the eukaryotic 40S ribosomal subunit in complex with initiation factor 1. Science 331: 730–736. https://doi.org/10.1126/science.1198308 PMID: 21205638

34. Choudhury K, Cardenas D, Pullikuth AK, Catling AD, Aiyar A, Kelly BL. (2011) Trypanosomatid RACK1 orthologs show functional differences associated with translation despite similar roles in *Leishmania* pathogenesis. PloS one 6: e20710. https://doi.org/10.1371/journal.pone.0020710 PMID: 21677780